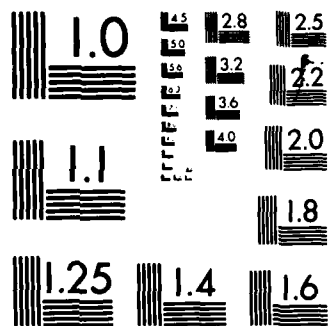


AD-A158 968 DEVELOPMENT OF HIGH SENSITIVITY X-RAY AND ELECTRON BEAM 1/1
RESIST PROCESSES(U) CALIFORNIA UNIV BERKELEY
ELECTRONICS RESEARCH LAB D W HESS MAY 85
UNCLASSIFIED AFOSR-TR-85-0738 F/G 9/5 NL

END

FILMED

DTIC



MICROCOPY RESOLUTION TEST CHART
NATIONAL BUREAU OF STANDARDS-1963-A

AD-A158 968

DTIC FILE COPY

SECURITY CLASSIFICATION OF THIS PAGE (When Data Entered)

②

REPORT DOCUMENTATION PAGE		READ INSTRUCTIONS BEFORE COMPLETING FORM
1. REPORT NUMBER AFOSR-TR-83-8	2. GOVT ACCESSION NO.	3. RECIPIENT'S CATALOG NUMBER
4. TITLE (and Subtitle) Development of High-Sensitivity X-ray and Electron Beam Resist Processes		5. TYPE OF REPORT & PERIOD COVERED Final Technical Report (12/15/79 - 1/29/85)
		6. PERFORMING ORG. REPORT NUMBER
7. AUTHOR(s) D. W. Hess		8. CONTRACT OR GRANT NUMBER(s) AFOSR 80-0078
9. PERFORMING ORGANIZATION NAME AND ADDRESS Electronics Research Laboratory University of California Berkeley, CA 94720		10. PROGRAM ELEMENT, PROJECT, TASK AREA & WORK UNIT NUMBERS 61102F, 2306, B2
11. CONTROLLING OFFICE NAME AND ADDRESS Air Force Office of Scientific Research Bldg. 410, Bolling Air Force Base Washington, DC 20332		12. REPORT DATE May 1985
		13. NUMBER OF PAGES 21
14. MONITORING AGENCY NAME & ADDRESS (if different from Controlling Office)		15. SECURITY CLASS (of this report) unclassified
		15a. DECLASSIFICATION/DOWNGRADING SCHEDULE
16. DISTRIBUTION STATEMENT (of this Report) unlimited Approved for unlimited distribution		
17. DISTRIBUTION STATEMENT (of the abstract entered in Block 20, if different from Report)		
18. SUPPLEMENTARY NOTES		
19. KEY WORDS (Continue on reverse side if necessary and identify by block number) High molecular weight studies, Spin Coating of Polymer Films, Resist Dissolution Studies		
20. ABSTRACT (Continue on reverse side if necessary and identify by block number) Investigations were performed under AFOSR Grant 80-0078 to study novel re- sists and related processes for use with e-beam and x-ray exposure systems. These studies concentrated on poly (methylmethacrylate) as an electron beam re- sist, since considerable previous information was available on this material. See next page		

DTIC
ELECTE
SEP 11 1985
S E D

Development of High Sensitivity X-Ray and
Electron Beam Resist Processes - Final Report (12/15/79-1/29/85)

Dennis W. Hess
Department of Chemical Engineering
University of California
Berkeley, California 94720

ABSTRACT

The lithographic performance of a polymer resist material is determined by several processes. First, uniform and controllable films of the resist must be reproducibly applied to the surface of substrates. Second, the radiation/polymer interaction is important since it affects the sensitivity of the resist. Third, the development or dissolution process is crucial because this step determines the ability to create useable patterns in the resist film. Finally, for Very Large Scale Integration (VLSI), dry etching processes are replacing liquid techniques; thus, the interaction of resists with glow discharges can often determine the utility of specific materials. Under AFOSR Grant 80-0078, various aspects of the above criteria were studied in order to gain fundamental understanding of these important process steps.

Using plasma-initiated polymerization, ultrahigh molecular weight ($>10^7$ g/mole) polymethylmethacrylate (PMMA) was formed and its utility as an e-beam resist studied. Although this material was degraded at a lower electron dose than conventional PMMA (MW = 7×10^5 g/mole), dissolution rates were low owing to the high MW even after scission. Further, pattern distortion was observed with the high MW material, apparently due to swelling and stress relief contraction as a result of the development cycle. Therefore, at this time, there appear to be practical limitations precluding the use of ultrahigh MW PMMA for VLSI.

A first-principles fluid dynamics model for the spin coating of PMMA has been developed. Non-Newtonian effects were taken into account by using a constitutive equation for the shear-rate dependent viscosity. Solution of this constitutive equation and the appropriate conservation equations yielded film thickness as a function of spin speed and initial viscosity. Results agreed quantitatively with experimental studies for solutions more concentrated than 3% of PMMA in chlorobenzene. Only qualitative agreement between theory and experiment was obtained for 2% PMMA solutions, apparently due to the neglect of surface forces in the model.

A partial ellipsometer (Psi meter) has been used to measure in-situ dissolution rates of PMMA in mixtures of methyl-ethyl ketone (MEK) and isopropyl alcohol (IPA). With higher concentrations of MEK (the "good" solvent), a fairly linear decrease in film thickness was observed. However, with increasing concentrations of IPA (the "poor" solvent), it appears that a gel layer may form at the polymer/solvent interface.

85 09 09 021

NOTES
THAT
DISC
MATERIALS
Chief, Technical Information Division

PMMA films were exposed to CF_4 and CF_4/O_2 discharges to ascertain the effect of plasmas on the degradation of PMMA. Successive layers of the exposed (and unexposed) films were removed and the molecular weight distribution measured. A small amount of degradation occurred throughout the entire film. However, the most severe degradation occurred near the top surface of the film. A statistical or probabilistic model was invoked to account for the results of this study. Agreement between theory and experiment suggested that the plasma degradation of PMMA occurred predominantly by a random scissioning process.

Accession For	
NTIS GRA&I	<input checked="checked" type="checkbox"/>
DTIC TAB	<input type="checkbox"/>
Unannounced	<input type="checkbox"/>
Justification	
By	
Distribution/	
Availability Codes	
Dist	Avail and/or Special
A-1	



Development of High-Sensitivity X-ray and
Electron Beam Resist Processes

Final Technical Report
AFOSR Grant 80-0078
(December 15, 1979 - January 29, 1985)

D. W. Hess
Principal Investigator

Department of Electrical Engineering and Computer Sciences
and the Electronics Research Laboratory
University of California
Berkeley, CA 94720

Introduction

Investigations were performed under AFOSR Grant 80-0078 to study novel resists and related processes for use with e-beam and x-ray exposure systems. These studies concentrated on poly (methylmethacrylate) as an electron beam resist, since considerable previous information was available on this material.

Background and Objectives

Throughout the last 20 years, the integrated circuit (IC) industry has steadily decreased the dimensions of the circuit elements fabricated in devices. Currently, production of circuits with minimum line widths of ~ 2 microns is performed by UV lithography. Continued reduction of geometries is advantageous because it permits the production of more complex and of faster circuits at reduced costs. However, as the dimensions decrease, diffraction effects become important, and the wavelength of the UV light becomes a limiting factor.

E-beam and x-ray lithography are promising techniques for the production of submicron devices. Since the wavelength of such radiation is on the order of angstroms, diffraction effects are negligible. In addition, direct wafer writing can be performed with electron beams, so a mask is not necessary.

In current and most future lithographic processes, polymers are used as resist materials. When these materials are exposed to radiation, some of their physical and/or chemical properties change. It is such changes that determine the ultimate usefulness of resists for fine-line pattern definition.

The lithographic performance of a polymer is determined by several processes. First, uniform and controllable films of the resist must be reproducibly applied to the surface of substrates. Second, the manner in which the polymer interacts with radiation is important because it affects the sensitivity of the resist. Third, the development or dissolution process is crucial because this

step determines the ability to create a usable pattern in the resist film. Fourth, the resolution of resist materials is intimately related to factors two and three above. Finally, since dry etching processes are replacing liquid techniques, the interaction of resists with glow discharges can often determine the utility of specific materials.

The goal of the following research on resist processing was to gain a fundamental understanding of the above processes which ultimately limit the lithographic performance of polymer resists. Our studies concentrated on the use of ultrahigh molecular weight polymers, the plasma degradation of polymer materials, and the modeling of spin coating processes.

High Molecular Weight Studies

Plasma-initiated polymerization has been used to form ultrahigh molecular weight (MW) polymers [1]. Due to the high MW, it was believed that such materials might display interesting properties insofar as sensitivity to radiation and solvent resistance are concerned. Indeed, theoretical studies [2-5] have suggested that the sensitivity of a resist can be increased either by increasing the $G(s)$ value (the number of mainchain scissions produced when the material absorbs 100 eV of energy) or by increasing the initial number of average molecular weight.

For plasma-initiated polymerization, methyl methacrylate (MMA) monomer was purified by vacuum distillation at 38°C. The purified monomer was then transferred (under vacuum) to a polymerization ampule [1]. The ampule was immersed in liquid nitrogen, and copper electrodes positioned on either side of the ampule stem. After warming the ampule until a pressure of 1 torr was established, an rf glow discharge was initiated in the tube between the electrodes. After one minute, the plasma was extinguished, the ampule was sealed and warmed to room temperature, and the monomer was mixed with the plasma

initiation products. The ampule was then shielded from light and placed in a water bath at 25°C for 24 hours. At the end of the polymerization period, the polymer that had formed was precipitated from the monomer solution, and was dissolved in methyl-ethyl-ketone (MEK).

The specific viscosity of various polymer solutions were measured using a low-shear Ubbelohde-type viscometer and by extrapolating this viscosity to infinite dilution, the intrinsic viscosity and thus the viscosity average molecular weight was determined. For comparison purposes, KTI PMMA electron beam resist was treated in the same manner, so that molecular weight determinations could be performed. The molecular weights obtained by this method were 3.1×10^7 g/mole for the plasma-initiated PMMA, and 6.9×10^5 g/mole for the KTI PMMA.

In order to determine the utility of the ultrahigh molecular weight (UHMW) PMMA as an electron beam resist, this material, dissolved in its monomer MMA, was spin-coated onto thermally oxidized silicon wafers and onto chromium-on-glass mask plates. For comparison, the KTI PMMA, which, as purchased, was dissolved in chloro-benzene, was spin-cast onto identical substrates. The thicknesses of both PMMA films were 0.42 μm .

Resist-coated samples were prebaked at 150°C for 30 minutes in a vacuum oven to improve chemical etch resistance and adhesion, and to drive off any residual monomer (UHMW) or solvent (KTI). No degradation of the polymer films was observed. In addition, both films were pinhole-free.

E-beam exposures were carried out in an ETEC Autoscan scanning electron microscope and in an ETEC MEBES-1 exposure system, using 10 KV electrons. Using a 1:1 mixture of MEK and isopropanol (IPA) as a developing solution, the dissolution rates of unexposed UHMW and KTI PMMA were 5 $\text{\AA}/\text{min}$. and 170 $\text{\AA}/\text{min}$., respectively. Finally, the SiO_2 and the chromium were etched with

buffered HF (1:7 HF:NH₄F) and chromium etch (Precision Photo Glass Chromium Etchant CR-8). Both resists adhered well during the etching of these two materials. Patterns were made with UHMW PMMA at doses of 3.2×10^{-6} C/cm² and 3.0×10^{-7} C/cm², respectively. At the lowest dose investigated (3.2×10^{-6} C/cm²), the 0.5 μ m lines were not clearly defined, but the 1 μ m were intact. At the highest dose studied (3.2×10^{-5} C/cm²), the 0.5 μ m were well defined, but the edges were a bit ragged.

With KTI PMMA, exposed at 3.2×10^{-6} C/cm², the lowest dose used for this polymer, an SEM picture indicated that the 0.5 μ m lines were very ragged and the unexposed regions were severely attacked. In fact, 40% of the unexposed resist was removed by the develop cycle. This is the reason that the KTI resist was not exposed at lower doses - significant thickness losses are incurred, and nonuniformities appear in the film during development times longer than a few minutes.

It should be noted that when higher exposure doses (3.2×10^{-5} C/cm²) were used KTI PMMA, sharp patterns of 0.5 μ m width could be generated, in agreement with previous studies using commercial PMMA. Such doses represent an increase of approximately a factor of 8 compared to comparable pattern formation in UHMW PMMA.

With the UHMW PMMA, dissolution rates of the unexposed resist were low, as discussed above. In addition, long development times were not necessary. At a dose of 3.2×10^{-6} C/cm², development times were ~ 2 min. This can be contrasted to the KTI PMMA, where the same dose required development times of ~ 4.5 min.

At low exposure doses ($< 10^{-6}$ C/cm²), UHMW PMMA spun onto wafers appeared unsuitable for submicron pattern definition. Apparently, a combination of swelling and stress relief contraction caused severe pattern distortion.

These effects arose because of the high MW of the PMMA. A low exposure dose means that the UHMW polymer fragments (after exposure) still have a high MW. Thus, relatively long (>2 min.) development time was needed. The unexposed polymer swelled during this time as indicated by SEM cross-sections of developed patterns. In addition, solvent molecules appeared to "lubricate" polymer molecules sufficiently to permit stress relief. This process caused contraction and thinning of the unexposed resist in regions up to 2 μm from the exposed areas. We believe that the high stress in UHMW polymers arose from the spinning process which left the long entangled polymer chains in a strained and nearly "extruded" state.

The resistance of the UHMW and KTI PMMA to plasma etching was briefly investigated. Patterned samples of each resist were exposed to a CCl_4 plasma at 0.1 torr and 0.3 W/cm² in a parallel plate plasma etcher for several minutes. Both resists were etched at $\sim 0.03 \mu\text{m}/\text{min.}$, and the resulting line dimensions were distorted.

Spin Coating of Polymer Films

The success of lithographic processes hinges in part on the reproducible generation of desired final resist film thicknesses and thickness uniformity. Many process variables influence the above film properties. As a result, attempts have been made to model the spin coating of silicon wafers with polymer resists. Literature exists that addresses this subject [6-13]. However, extensive fundamental work had not yet been done to firmly establish the relationships between all process variables and film thickness and uniformity. Thus, a general model of polymer spin coating was needed.

Our approach to spin modeling has been described in a recent publication [14], so that only a simplified discussion will be presented here. If the rotating axis of the wafer is taken as the Z axis of the cylindrical coordinate system used

in the model, both the concentration profile of the resist solution, $c(t,r,z)$, and the velocity field, $v(t,r,z)$, possess r and z dependence but no ϑ -dependence due to the inherent symmetry of the problem. The dynamic equations, i.e., equation of motion and mass transport can be easily written [15]. These equations are general and independent of the material under study. However, reliable constitutive equations correlating the viscosity and diffusivity with the concentration and molecular weight must be substituted into the dynamic equations to permit solution of the thickness variation as a function of processing time and radial position. A modified version of the Doolittle equation [16], based on the free volume concept, is adopted here to accommodate the concentration dependence of diffusivity and viscosity, whereas the molecular weight dependence of viscosity follows that given by scaling concepts [17]. The origin of the coordinate system lies on the disk (wafer) surface along the axis of rotation. The overall system is characterized by the disk radius and the angular rotation speed. Film thickness is a function of radial distance. Naturally, the thickness changes with time during spinning. Major assumptions for this modeling effort are summarized below.

1. Fluid flow is rotationally symmetrical. This assumption removes angular dependence in the ensuing analysis.
2. Velocity is restricted to the r -direction only. This lubrication approximation greatly simplifies the equations of continuity and motion. Since the thickness does not depend on radial position strongly, this assumption is reasonably sound.
3. Surface forces are neglected. Often the fluid piles up around the edges of the disk due to surface tension. However, this ring around the edges is narrow compared to the rest of the surface, where topography is not much perturbed by the existence of the ring. We therefore limit our analysis to the

large central flat region of the disk away from the edges.

4. Density of the fluid stays constant. In fact, the polymer and solvent are assumed to have the same density. Thus, composition variation does not lead to density change, and weight fraction is equivalent to volume fraction in our analysis.
5. During the process, fluid temperature and partial vapor pressure of the solvent in the spinner chamber remain constant. Note that a simple order-of-magnitude calculation of energy balance and rate of heat transfer confirms that evaporation of solvent in a thin film does not lead to a significant temperature change in the film.

Solutions of the appropriate conservation and constitutive equations subject to the above assumptions yield predictions of film thickness as a function of spin speed and initial viscosity. Results are obtained by using a similarity transformation to solve for the concentration profile, and a fourth-order Runge-Kutta method to obtain velocity profiles. Although the trends are qualitatively identical to those observed experimentally, quantitative deviations between theory and experiment remain. The model predicts a thicker film than observed experimentally. When the rotational speed is high, the fluid is sheared to a large extent, inducing appreciable shear thinning of the material. Hence, approximation of the fluid behavior by a Newtonian constitutive equation leads to inaccurate predictions. Further, the Newtonian model yields too weak a film thickness dependence on spinner speed. These deficiencies have been overcome by expanding the initial analysis to include non-Newtonian features of the resist solution.

To accommodate non-Newtonian effects, a realistic constitutive equation is used for the shear-rate dependent viscosity [18-20]. The overall system viscosity is divided into contributions from the polymer and remaining solvent:

$$\eta = \eta_p + \eta_s = \frac{\eta_{po}}{1+b\dot{\gamma}^a} + \eta_s \quad (1)$$

where η is the total system viscosity, η_p and η_s are the polymer and solvent contributions, b and a are parameters characterizing the onset of non-Newtonian behavior and the slope of the power-law relationship for the shear-rate, $\dot{\gamma}$, dependence. The quantity η_{po} is the polymer contribution to the viscosity at zero shear and is described by Equation (2).

$$\eta_{po} = kc^m \exp\left(\frac{B}{f}\right) \quad (2)$$

where c is the polymer concentration, B is a constant of order unity, f is the fractional free volume [21] at the given temperature and concentration, and k and m are material constants.

Experimental results and model predictions based on the non-Newtonian analysis are summarized on a log-log plot of average film thickness as a function of the final spin speed (Figure 1). Excellent agreement is seen between the model predictions and experimental data for 9,6, and 4% resist solutions. Serious discrepancy occurs, however, for the 2% polymer solution, the calculated thickness being significantly thicker than the experimental values. (Still, the slope of the predicted curve is in agreement with the data). The most likely source of this error is neglect of surface forces in the model. A 2% polymer solution spun at 1,000 rpm leaves a final film that is approximately 200 nm thick, corresponding to only a few monolayers of polymer. The failure to model the spin coating of films from a 2% solution is not a serious problem since solutions with a polymer weight fraction below about 4% are generally not used in commercial practice. The reason for this is that very thin films often contain a large number of pinholes.

References

- [1] L. M. Gavens, B. J. Wu, D. W. Hess, A. T. Bell, and D. S. Soong, *J. Vac. Sci. Technol.*, **B1**, 481 (1983).
- [2] M. J. Bowden, *CRC Critical reviews in Solid State and Materials Sciences*, **8**(3), 223 (1979).
- [3] A. Charlesby, *Atomic Radiation and Polymers*, Pergamon Press, Oxford, 1960.
- [4] M. Hatsakis, C. H. Ting, and N. Viswanathan, "Electron and Ion Beam Science and technology," 8th International Conference, p. 542, Nov. 1974.
- [5] F. Asumussen and K. Ueberreiter, *J. Polym. Sci.*, **57**, 199 (1962).
- [6] A. Acrivos, M. J. Shah and E. E. Petersen, *J. Appl. Phys.*, **31**, 963 (1960).
- [7] G. F. Damon, "Kodak Seminar on Microminiaturization," 1969, p. 195.
- [8] W. J. Daughton and F. L. Givens, *J. Electrochem. Soc.*, **129**, 173 (1982).
- [9] L. A. Dorfman, *J. Eng. Phys.*, **12**, 309 (1967).
- [10] A. G. Emslie, F. T. Bonner, C. G. Peck, *J. Appl. Phys.*, **29**, 858 (1958).
- [11] F. L. Givens and W. J. Daughton, *J. Electrochem. Soc.*, **126**, 269 (1979).
- [12] D. Meyerhofer, *J. Appl. Phys.*, **49**, 3393 (1978).
- [13] B. D. Washo, *IBM, J. Dev. Develop.*, **21**, 90 (1977).
- [14] W. W. Flack, D. S. Soong, A. T. Bell and D. W. Hess, *J. Appl. Phys.*, **56**, 1199 (1984).
- [15] R. B. Bird, W. E. Stewart, and E. N. Lightfoot, "Transport Phenomena," Wiley and Sons, N.Y., 1960.
- [16] A. K. Doolittle and D. B. Doolittle, *J. Appl. Phys.*, **31**, 1164 (1959).

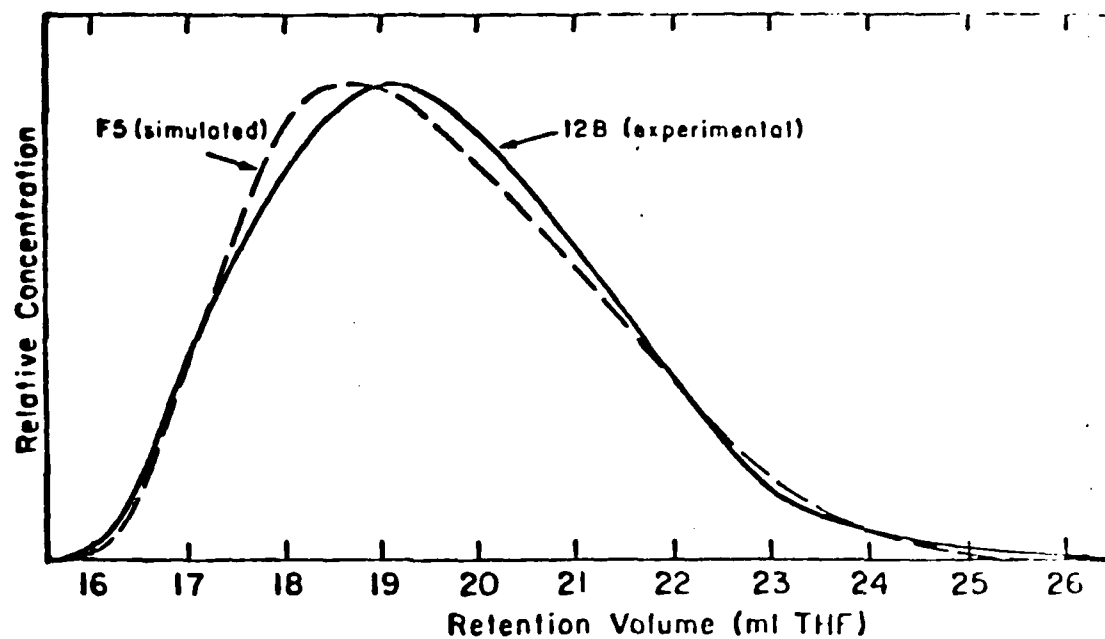


Fig. 9. Comparison of simulated and experimental GPC traces for middle section of PMMA film (See Fig. 5).

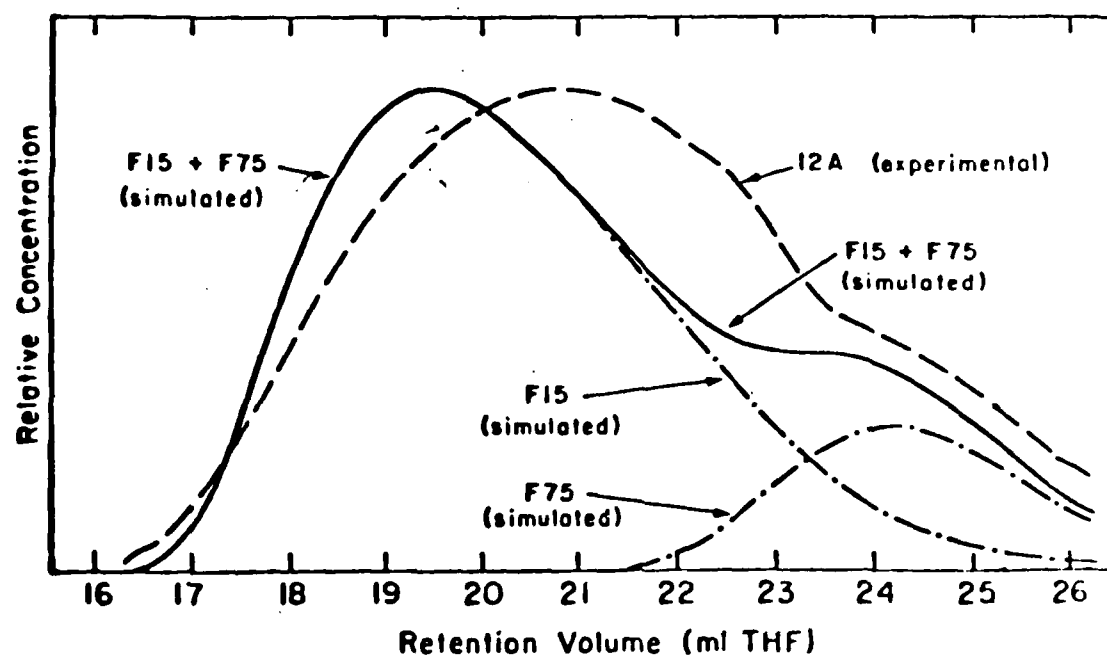


Fig. 10. Comparison of simulated and experimental GPC traces for the top of the PMMA films (See Fig. 5).

ures 9 and 10. (Details of the model can be found in Ref. [26]). Clearly, good agreement is obtained for the regions of the film furthest removed from the plasma. However, at the film surface, where significant ion and electron bombardment occur, the simple random scissioning gives only a qualitative agreement. Apparently, the polymer molecules undergo varying degrees of degradation, as indicated by the fact that a broadened molecular weight distribution with two discernible "peaks" is observed (Figure 10).

The results of the degradation experiments suggest that the plasma degradation of PMMA occurs predominantly by a random scissioning model, as proposed by Harada [25]. Further, the degradation occurs in a similar manner to that due to e-beam exposure [27]. Finally, the fact that most of the degradation occurs within the top third (or less) of the film indicates that a surface hardening or conversion treatment may be all that is required to protect the resist against dry etching processes.

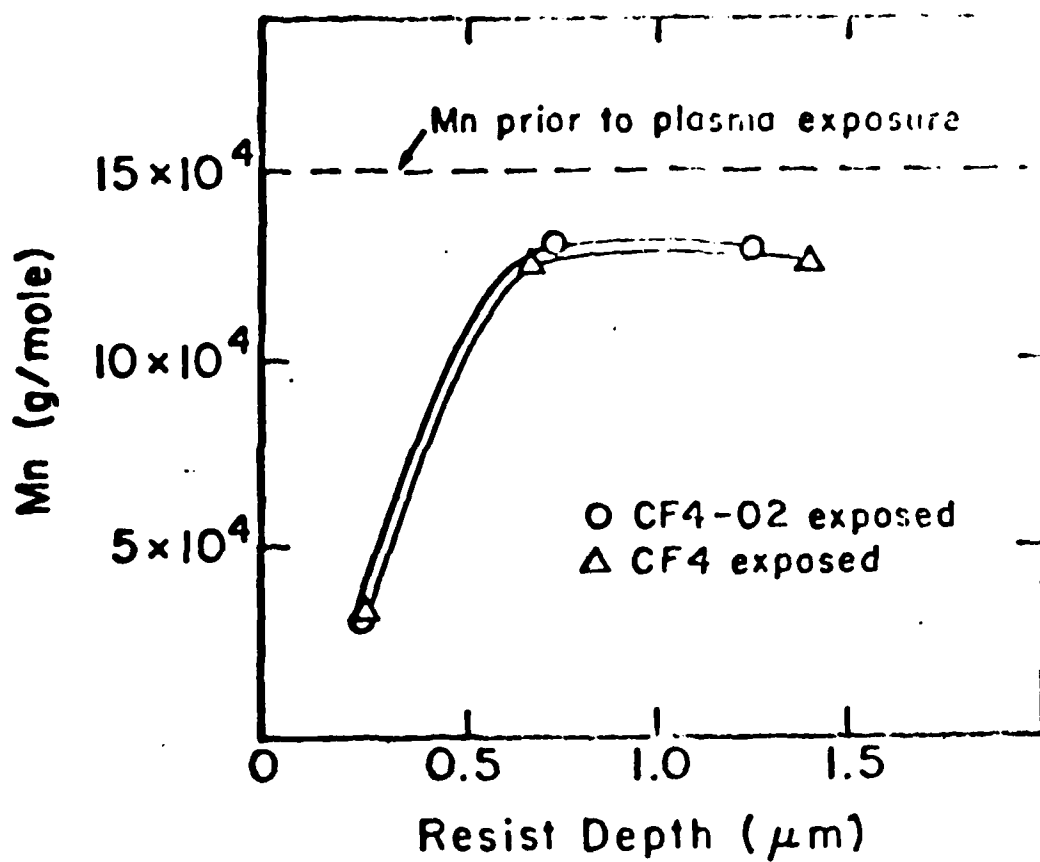


Fig. 8. PMMA molecular weight versus resist depth after plasma exposure

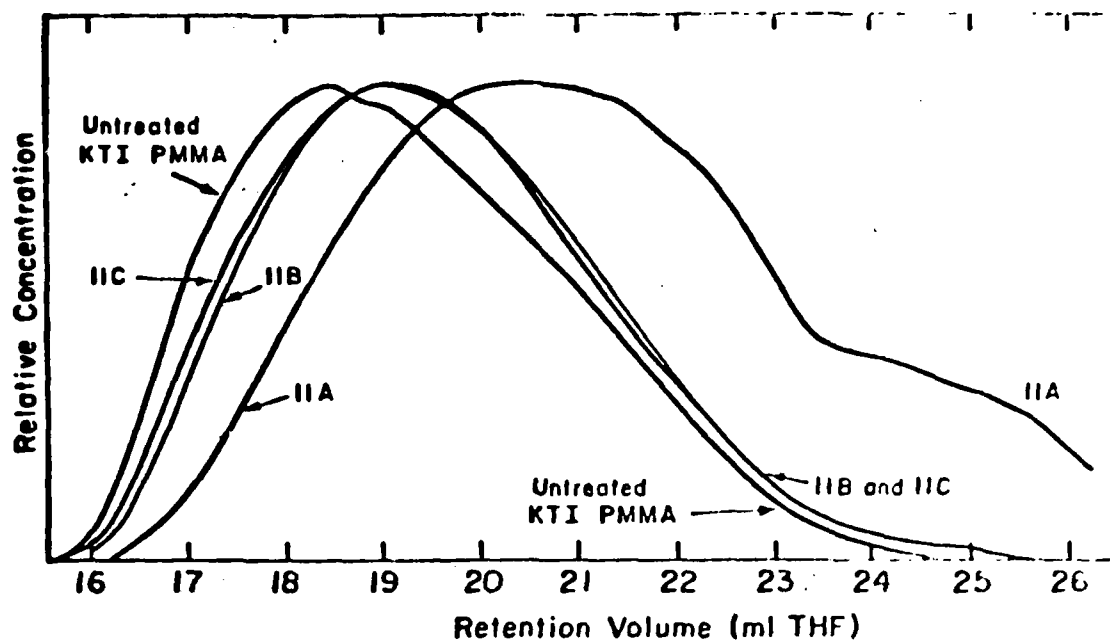


Fig. 6. GPC traces for CF_4/O_2 exposed PMMA films. Trace designations correspond to the profiling scheme of Fig. 5.

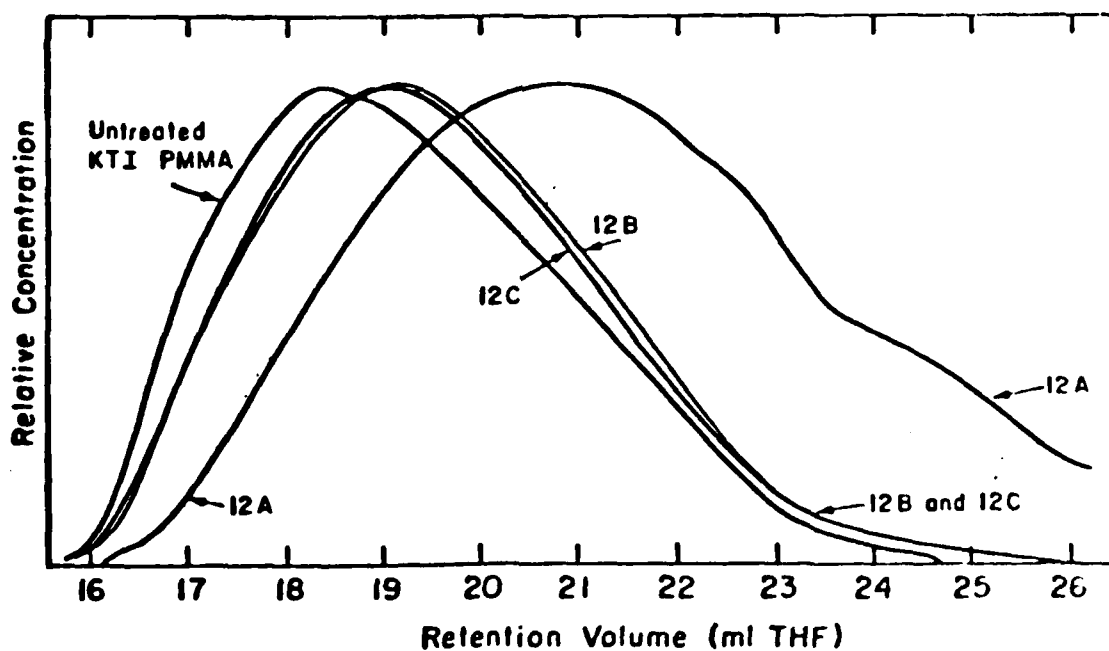


Fig. 7. GPC traces for CF_4 exposed PMMA films. Trace designations correspond to the profiling scheme of Fig. 5.

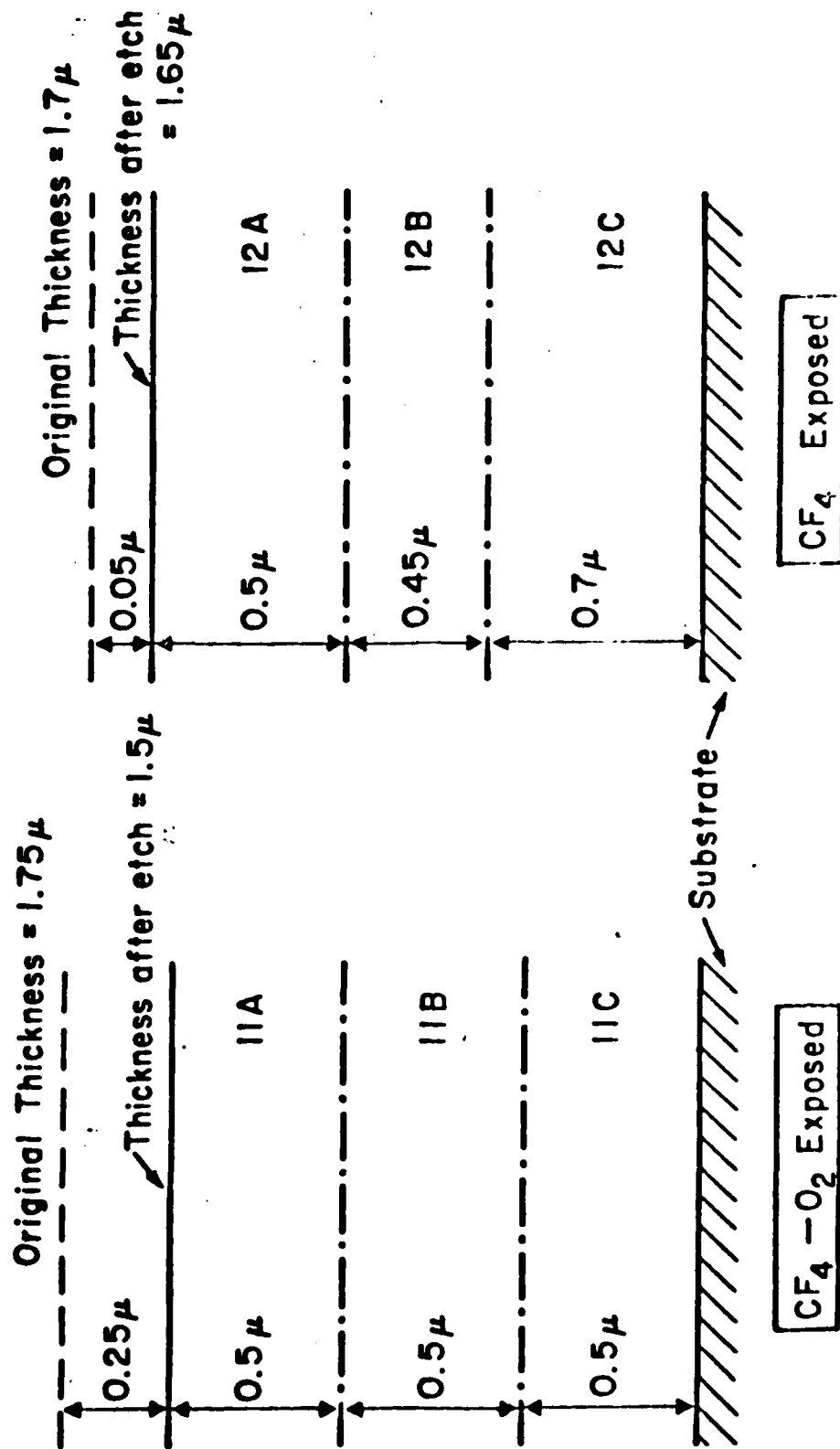


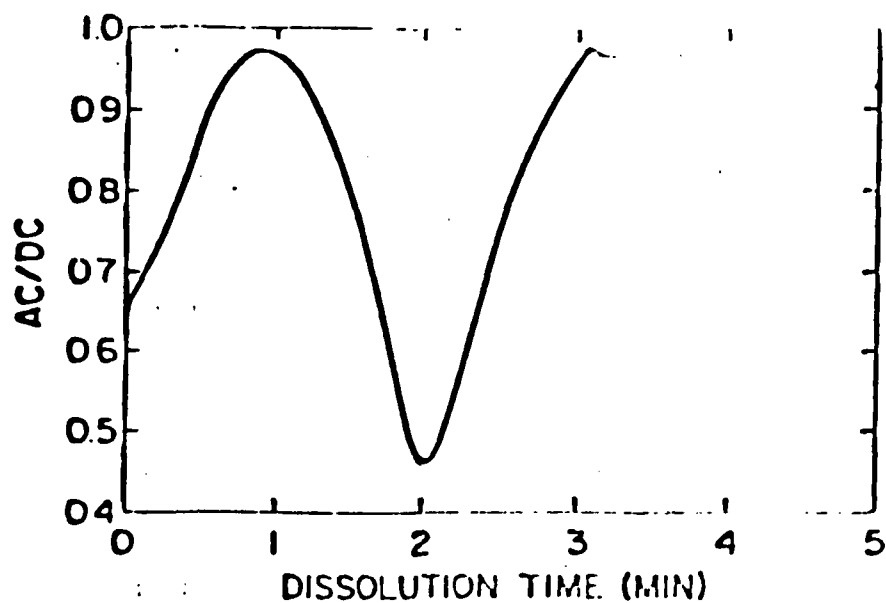
Fig. 5 GPC resist profiling scheme for plasma-exposed PMMA films.

PMMA Degradation Studies

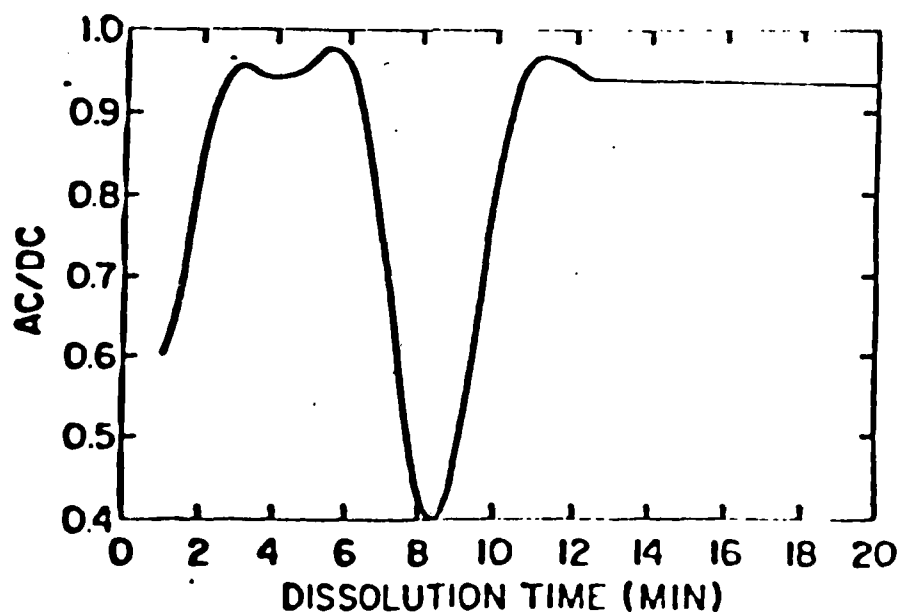
In order to understand the degradation of resist materials in rf glow discharges used for etching, and thus to generate insight into plasma-resistant resist processes, poly(methyl methacrylate) (PMMA) was exposed to CF_4 and to $\text{CF}_4/8\% \text{O}_2$ plasmas. The exposures were carried out in a parallel plate plasma reactor at 4.5 MHz with an rf power density of 0.2 W/cm^2 , and a pressure of $300 \mu\text{m}$ for 5 min. A direct indication of the extent of degradation was obtained by comparing the molecular weight distribution of PMMA before and after plasma exposure. Successive layers of the exposed (and unexposed) films were removed by immersion in tetrahydrofuran. Each layer was analyzed for molecular weight distribution by gel permeation chromatography (GPC).

The profiling scheme for CF_4 and for CF_4/O_2 plasma exposure is shown in Figure 5. With both etch gases, the original resist thickness decreases due to plasma exposure. Figures 6 and 7 show GPC traces corresponding to the etch scheme indicated by Figure 5. The experimentally obtained molecular weight distribution for untreated PMMA (KTI "950 K") is also shown in Figures 6 and 7. From these figures, it can be seen that a small amount of degradation occurs throughout the thickness of the resist film. However, the most severe degradation occurs in the top third of the film. This can be seen more clearly by computing a molecular weight distribution from the GPC data. These results are shown in Figure 8. Clearly, the degradation profiles for CF_4 and CF_4/O_2 plasma-exposed films are 100 and 500 \AA min , respectively. This suggests that the effect of O_2 additions may be confined to the surface of the resist, thereby merely enhancing the chemical etch rate.

The observed degradation of PMMA was modeled by using statistical or probabilistic methods, since random chain scissioning is believed to be the dominant degradation mechanism [25]. The results of this model are shown in Fig-



(a)



(b)

Fig. 4. Amplitude ratios of the AC to DC components as functions of time for PMMA dissolution in MEK and IPA developer solutions with compositions (volume ratios of MEK to IPA) of 6:4 and 4:6.

wavelength of the light, incidence angle and film thickness through the Drude equation [23].

Silicon wafers coated with approximately 700 nm PMMA resist and prebaked at 180° for one hour were used in this study. Film dissolution took place in the optical cell, where a developer solution at room temperature was circulated at 100 ml per minute with the aid of an external pump. The optical cell has a capacity of 250 ml. The motor-driven polarizer was adjusted to a rotation frequency of 100 Hz. An incident angle of 75° was chosen to maximize sensitivity. The wavelength was 632.8 nm. Data were collected at a rate of one point per second, allowing detailed delineation of the dissolution phenomenon.

Figure 4 shows plots of AC/DC amplitude ratios as a function of dissolution time for wafers immersed in developer solutions of methyl ethyl ketone (MEK) and isopropanol (IPA) with different compositions. Appreciably different time scales are needed to achieve dissolution, with shorter development times for solutions of greater strengths (higher concentrations of MEK, the good solvent). The curve for the stronger developer solution, after deconvolution by a program attributed to McCrackin [24], indicates a fairly linear decrease in film thickness with time, with no appreciable induction period and no distinct multiple layer formation. An extra maximum, however, emerges in the AC/DC at short times for the weaker solution. This intriguing observation leads to several possible hypotheses to rationalize its existence. At present, we suspect that this extra maximum is associated with the formation of a gel layer at the solution-resist interface. Polymer dissolution involves first solvent penetration into the glassy matrix, converting it into a rubbery gel phase, followed by a detachment of chain molecules from the entangled gel network into the solution. The former process is influenced by the mobility of small solvent molecules penetrating the glassy phase, whereas the latter is affected by chain diffusion.

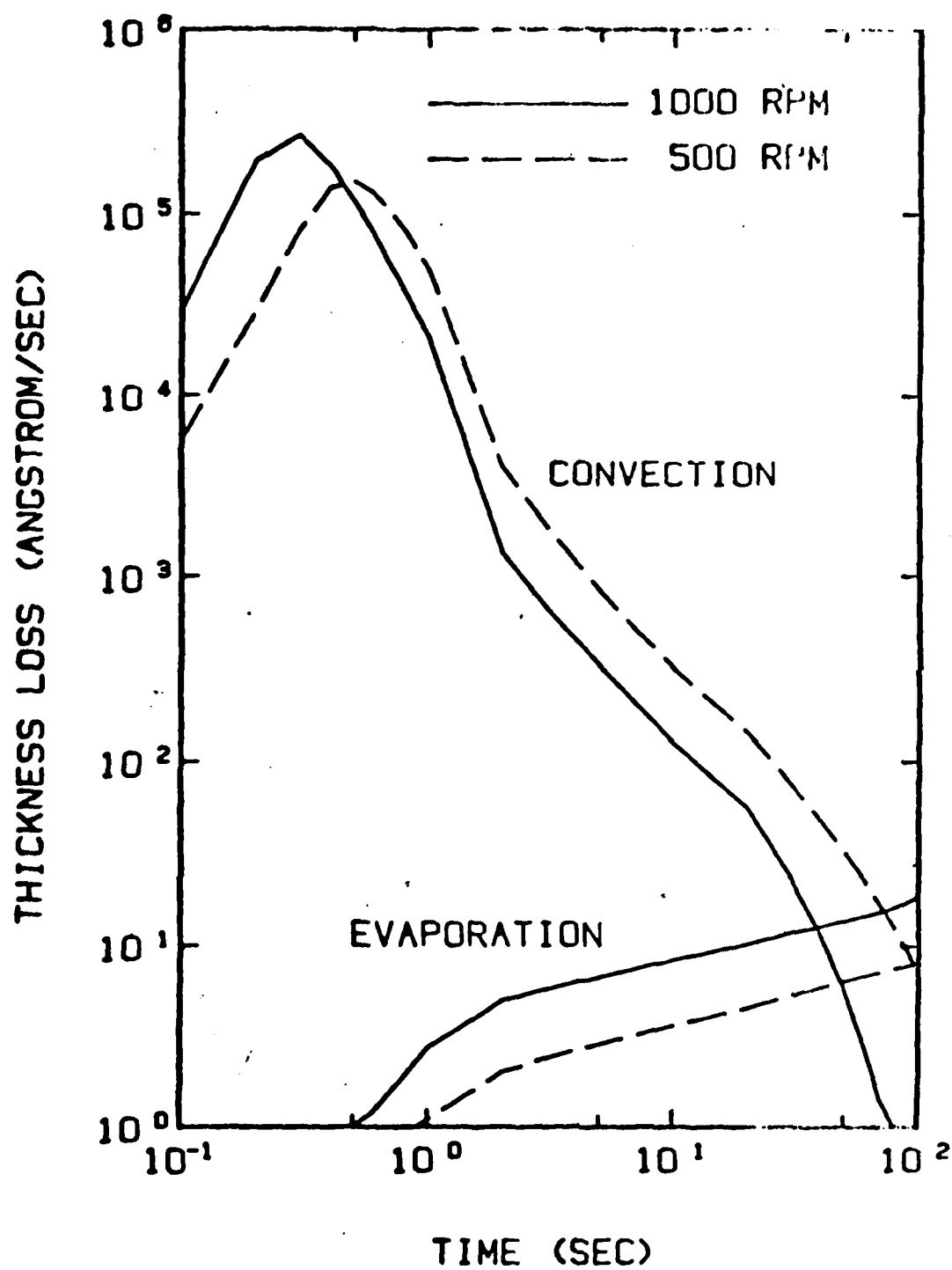


Fig. 3. Model results showing the effects of spin speed on thickness loss rate as a function of time.

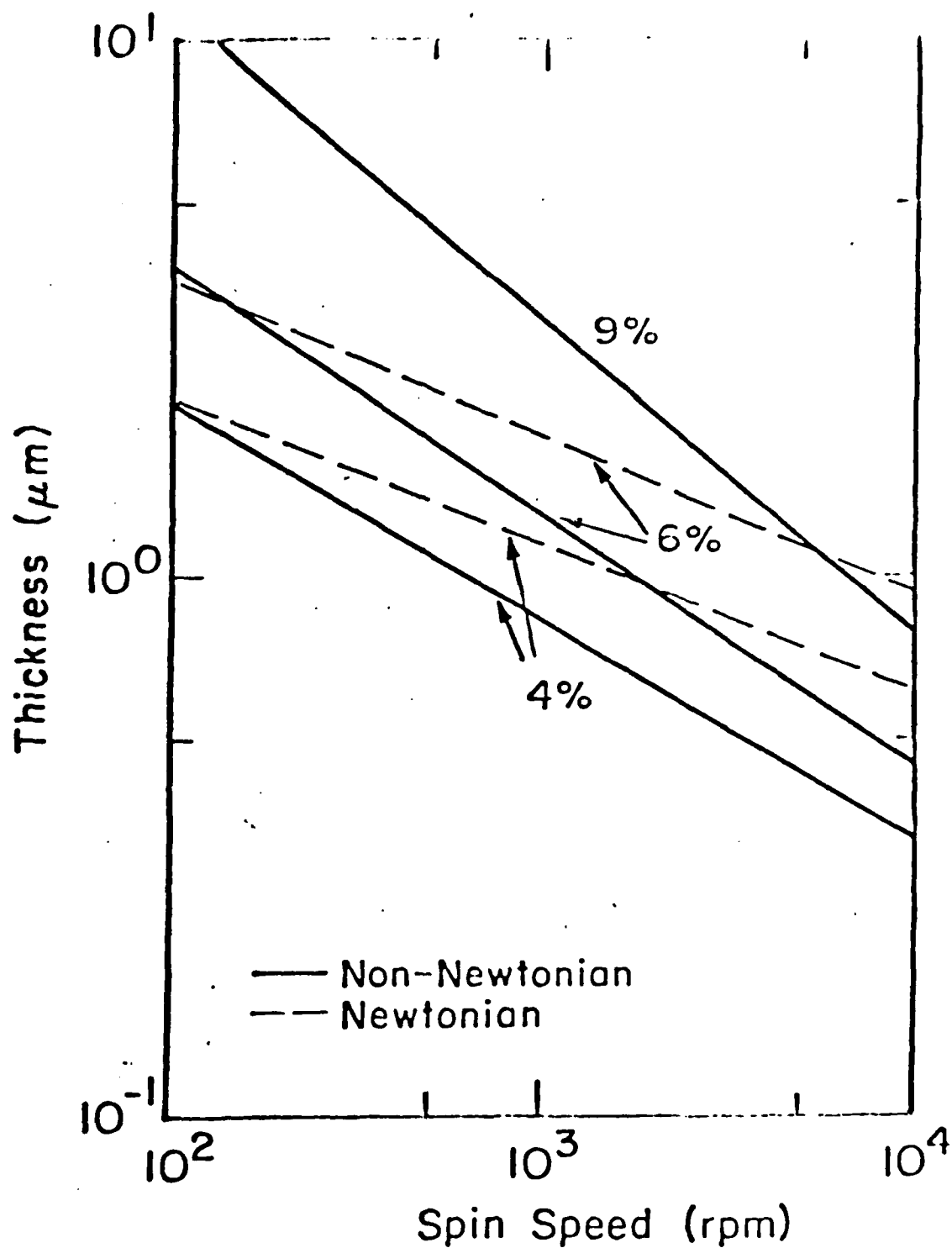


Fig. 2 Calculated film thickness as a function of spin speed and concentration. Solid curves represent the non-Newtonian analysis, while dotted curves are for the Newtonian model. Neglect of shear-thinning behavior not only results in overpredictions of film thickness but also underprediction of its dependence on spin speed.

The significance of the non-Newtonian characteristics of the resist solution is illustrated in Figure 2. It is apparent that the assumption of Newtonian behavior leads to a weaker dependence of film thickness on spin speed than is observed experimentally, and one which is independent of polymer concentration in the initial resist. The non-Newtonian model not only gives quantitative predictions of the film thickness, but also generates the correct dependence on spinner speed. The dependence on spinner speed is stronger for the higher concentration solutions. This is attributable to the more prominent non-Newtonian behavior of the resist at higher concentrations.

The evolution of film thickness during a given process is analyzed on a time basis in Figure 3. Here, film thickness reduction due to convective motion dominates at short times, whereas solvent loss due to evaporation takes over at long times when the film is thin and the fluid viscosity becomes high.

Resist Dissolution Studies

In order to fundamentally understand and model the resist development process, accurate and extensive data on the change in film thickness as a function of time in solvent solutions are needed. To obtain such information, we have used a psi-meter (partial ellipsometer) to investigate dissolution phenomena [22]. Briefly, the psi-meter consists of a 2 mW helium-neon polarized laser source, a quarter wave retardation plate to generate circularly polarized light, and a synchronously rotating polarizer to convert the beam to linearly polarized light with time-dependent orientation. Light reflected from the wafer placed in the optical cell enters a photodetector. The signal from the detector is split into AC and DC components by the ratio-meter. Final data acquisition and storage are achieved with a dedicated Commodore PET 2001 computer.

The amplitude ratio of the AC to DC components is equal to $-\cos(2\psi)$, and ψ is related to the optical constants of the substrate, film, and ambient, the

The significance of the non-Newtonian characteristics of the resist solution is illustrated in Figure 2. It is apparent that the assumption of Newtonian behavior leads to a weaker dependence of film thickness on spin speed than is observed experimentally, and one which is independent of polymer concentration in the initial resist. The non-Newtonian model not only gives quantitative predictions of the film thickness, but also generates the correct dependence on spinner speed. The dependence on spinner speed is stronger for the higher concentration solutions. This is attributable to the more prominent non-Newtonian behavior of the resist at higher concentrations.

The evolution of film thickness during a given process is analyzed on a time basis in Figure 3. Here, film thickness reduction due to convective motion dominates at short times, whereas solvent loss due to evaporation takes over at long times when the film is thin and the fluid viscosity becomes high.

Resist Dissolution Studies

In order to fundamentally understand and model the resist development process, accurate and extensive data on the change in film thickness as a function of time in solvent solutions are needed. To obtain such information, we have used a psi-meter (partial ellipsometer) to investigate dissolution phenomena [22]. Briefly, the psi-meter consists of a 2 mW helium-neon polarized laser source, a quarter wave retardation plate to generate circularly polarized light, and a synchronously rotating polarizer to convert the beam to linearly polarized light with time-dependent orientation. Light reflected from the wafer placed in the optical cell enters a photodetector. The signal from the detector is split into AC and DC components by the ratio-meter. Final data acquisition and storage are achieved with a dedicated Commodore PET 2001 computer.

The amplitude ratio of the AC to DC components is equal to $-\cos(2\psi)$, and ψ is related to the optical constants of the substrate, film, and ambient, the

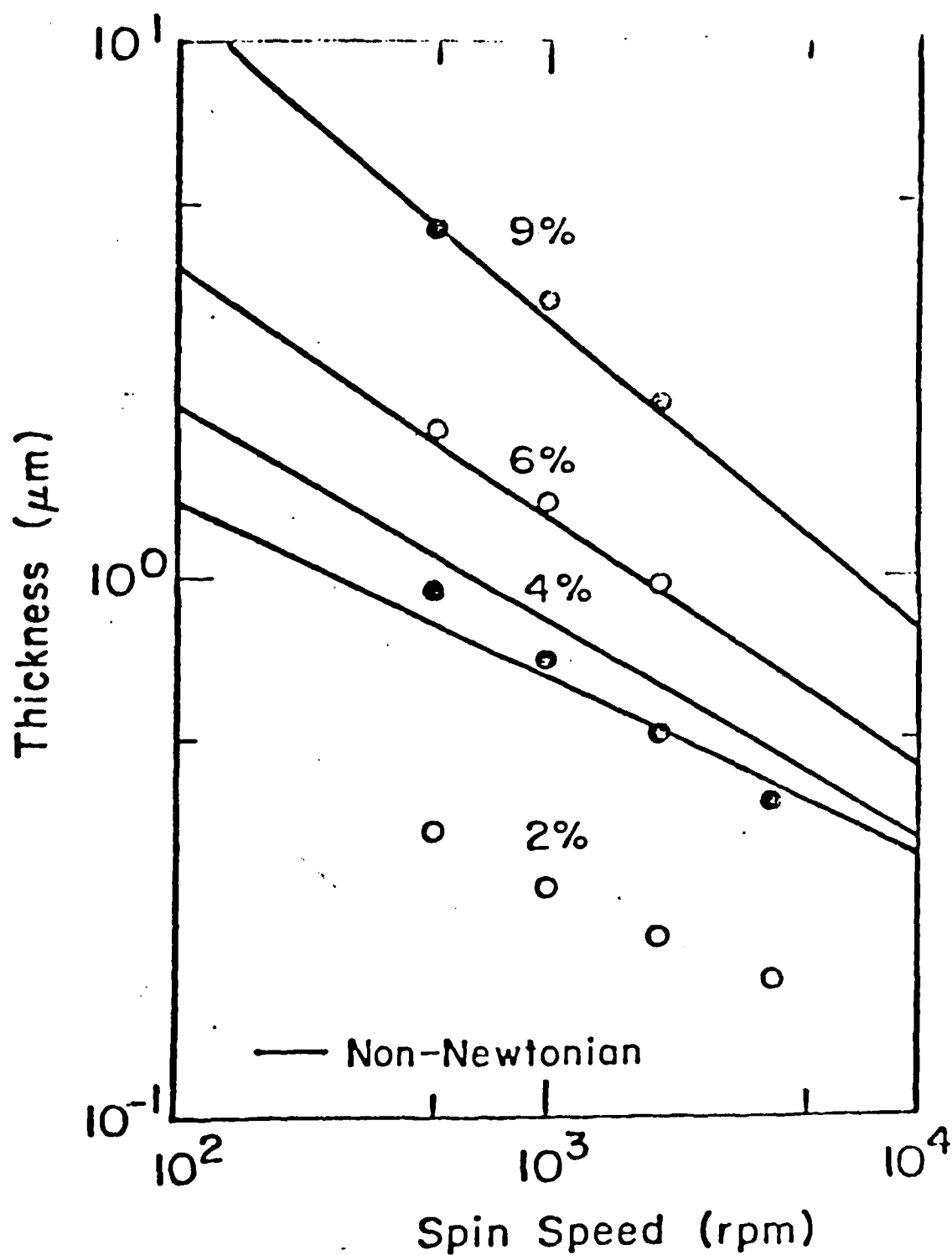


Fig. 1 Comparison of measured and predicted average film thickness as a function of final spin speed for several resist concentrations. Increasing speed decreases film thickness, whereas increasing initial solution concentration leads to thicker deposits. Model predictions agree well with experimental observations for reasonably concentrated solutions. At low initial concentrations, e.g., 2% to 4%, the model overpredicts the final film thickness.

- [17] P. de Gennes, "Scaling Concepts in Polymer Physics," Cornell University Press, Ithaca, N.Y., 1979.
- [18] D. S. Soong and M. Shen, *J. Rheol.* **25**, 259 (1981).
- [19] T. Y. Liu, D. S. Soong, and M. C. Williams, *Polym. Eng. Sci.*, **21**, 675 (1981).
- [20] T. Y. Liu, D. S. Soong and M. C. Williams, *J. Rheology*, **27**, 7 (1983).
- [21] M. L. Williams, R. F. Landel and J. D. Ferry, *J. Am. Chem. Soc.*, **77** 3701 (1955).
- [22] W. W. Flack, J. S. Papanu, D. W. Hess and D. S. Soong, *J. Electrochem. Soc.*, **131**, 2200 (1984).
- [23] R. Azzam and N. Bashara, *Ellipsometry and Polarized Light*, North Holland Publishing Company, N.Y., 1977.
- [24] F. McCrackin, "A Fortran Program for Analysis of Ellipsometer Measurements," NBS Technical Note 497 (1969).
- [25] K. Harada, *J. Appl. Polym. Sci.*, **26**, 1961 (1981).
- [26] B. J. Wu, D. W. Hess, D. S. Soong and A. T. Bell, *J. Appl. Phys.*, **54**, 1725 (1983).
- [27] J. Lai and L. Shepherd, *J. Appl. Polym. Sci.*, **20**, 2367 (1976).

END

FILMED

10-85

DTIC